

Computational Study on Kinetics and Mechanisms of Unimolecular Decomposition of Succinic Acid and Its Anhydride

Hsin-Tsung Chen,^{†,§} Jee-Gong Chang,^{†,‡} Djmaladdin G. Musaev,^{*,†} and M. C. Lin^{*,†,§}

Cherry L. Emerson Center for Scientific Computation, and Department of Chemistry, Emory University, Atlanta, Georgia 30322, National Center for High-performance Computing, No. 28, Nan-Ke 3rd Road, Hsin-Shi, Tainan 744, Taiwan, and Center for Interdisciplinary Molecular Science, National Chiao Tung University, Hsinchu 300, Taiwan

Received: March 5, 2008; Revised Manuscript Received: May 5, 2008

The mechanisms and kinetics of unimolecular decomposition of succinic acid and its anhydride have been studied at the G2M(CC2) and microcanonical RRKM levels of theory. It was shown that the ZsgsZ conformer of succinic acid, with the Z-acid form and the gauche conformation around the central C–C bond, is its most stable conformer, whereas the lowest energy conformer with the E-acid form, ECGsZ, is only 3.1 kcal/mol higher in energy than the ZsgsZ. Three primary decomposition channels of succinic acid producing H₂O + succinic anhydride with a barrier of 51.0 kcal/mol, H₂O + OCC₂H₃COOH with a barrier of 75.7 kcal/mol and CO₂ + C₂H₅COOH with a barrier of 71.9 kcal/mol were predicted. The dehydration process starting from the ECGCZ-conformer is found to be dominant, whereas the decarboxylation reaction starting from the ZsgsZ-conformer is only slightly less favorable. It was shown that the decomposition of succinic anhydride occurs via a concerted fragmentation mechanism (with a 69.6 kcal/mol barrier), leading to formation of CO + CO₂ + C₂H₄ products. On the basis of the calculated potential energy surfaces of these reactions, the rate constants for unimolecular decomposition of succinic acid and its anhydride were predicted. In addition, the predicted rate constants for the unimolecular decomposition of C₂H₅COOH by decarboxylation (giving C₂H₆ + CO₂) and dehydration (giving H₃CCHCO + H₂O) are in good agreement with available experimental data.

Introduction

Succinic acid (SA), also called amber acid or butanedioic acid, is one of the dicarboxylic acids with the molecular formula of C₄H₆O₄ and was first purified from amber by Georgius Agricola in 1546. It has been produced by microbial fermentation for the use in agricultural, food and pharmaceutical industries.¹ Commercially, SA is synthesized from liquefied petroleum gases (LPG) or petroleum oil. SA is also found in samples of atmospheric aerosol particles,² which affect quality of life³ and the Earth's radiative forcing.⁴ SA has been widely used as a precursor of many industrially important chemicals including adipic acid, 1,4-butanediol, tetrahydrofuran, N-methylpyrrolidinone, 2-pyrrolidinone, succinate salts and γ -butyrolactone.⁵ Recently, SA has been employed as an anti-ablative material for boundary layer control system (BLCS) in high-pressure graphite rocket nozzle.⁶ However, the thermal statistics of SA and kinetics for its unimolecular decomposition are still unknown. It is also imperative to understand the high-temperature products of SA decomposition in a rocket propulsion system.

Previously, the conformational complexity of SA has been studied at ab initio and OPLS-AA levels of theory by Price et al.⁷ It was shown that the ZsgsZ conformer (see Figure 1), its Z-acid form with a gauche conformation around the central C–C bond, is the lowest energy conformer of SA. Its lowest energy conformer with an E-acid group and an internal hydrogen-bond

is about 3 kcal/mol higher in energy. However, in the literature there are no quantitative interpretations (both experimentally and theoretically) of the decomposition of the SA and its anhydride. Therefore, the present work is the first attempt on comprehensive studies of both conformational complexity and unimolecular decomposition mechanisms of SA and its anhydride. Here, we also predict the rate constants of all elementary reactions involved in the decomposition of SA.

Computational Methods

The geometries of the reactants, intermediates, transition states and products for succinic acid and its anhydride decomposition reactions in the gas phase have been optimized at the B3LYP/6-311+G(d,p) level of theory.^{8–10} The vibrational frequencies were calculated at the same level of theory to characterize the nature of the stationary points of the reported potential energy surfaces (PES) and to include zero-point energy (ZPE) corrections in the reported energetics. Intrinsic reaction coordinate (IRC)¹¹ calculations were performed to connect each reported transition state with the associated reactants and products. To obtain more accurate energies and rate constants, we performed a series of single-point energy calculations for each stationary points of PESs with the modified GAUSSIAN-2 method,¹² the G2M(CC2), which is based on the B3LYP/6-311+G(d,p) optimized geometries. The G2M(CC2) composite scheme is as follows:

$$E[\text{G2M(CC2)}] = E_{\text{bas}} + \Delta E(+3\text{df}2\text{p}) + \Delta E(\text{CC}) + \Delta E(\text{HLC,CC2}) + \text{ZPE}$$

$$\text{where } E_{\text{bas}} = E[\text{PMP4(SDTQ)/6-311G(d,p)}]$$

* Corresponding authors. E-mail: M.C.L., chemmcl@emory.edu; D.G.M., dmusaev@emory.edu.

[†] Emory University.

[§] National Chiao Tung University.

[‡] National Center for High-performance Computing.

$$\Delta E(+3df2p) = E[\text{MP2}/6-311+\text{G}(3df,2p) - \text{MP2}/6-311\text{G}(\text{d,p})]$$

$$\Delta E(\text{CC}) = E[\text{CCSD}(\text{T})/6-311\text{G}(\text{d,p}) - \text{PMP4}(\text{SDTQ})/6-311\text{G}(\text{d,p})]$$

The higher level corrections, $\Delta E(\text{HLC}, \text{CC2})$, are given by $-5.3n_\beta - 0.19n_\alpha$ in milli-hartree, where n_α and n_β are the numbers of α and β valence electrons, respectively. All calculations were performed by Gaussian_2003 quantum chemical package.¹³

The microcanonical Rice–Ramsperger–Kassel–Marcus (RRKM) theory^{14–17} was employed to calculate the rate constants for the unimolecular decomposition reactions of succinic acid and its anhydride by the *ChemRate* code.¹⁸

Results and Discussion

The optimized structures of the rotational conformers of SA are shown in Figure 1. The relative energies and the three

dihedral angles ($D1$ or $D3$, and $D2$) of the predicted conformers are presented in Table 1. Schematic energy change upon changing dihedral angles ($D1$, $D2$, and $D3$) from -180° to $+180^\circ$ by increments of 10° and optimizing all other geometries of the systems are depicted in Figure 2. In Figures 3 and 4 we present structures and geometries of the located intermediates, transition states and products of the unimolecular succinic acid decomposition reactions, and Figure 5 includes relative energies of these structures. Predicted first-order rate constants (in unit of s^{-1}) for succinic acid and its anhydride decomposition in the temperature range 300–3000 K are shown in Figure 6.

1. Conformation of Succinic Acid (SA). Here we investigate the possible rotational conformers of SA. The internal rotational angles are schematically presented in Scheme 1.

Internal rotations around the $\text{C}^1\text{--}\text{C}^2$, $\text{C}^2\text{--}\text{C}^3$, and $\text{C}^3\text{--}\text{C}^4$, called below as D_1 , D_2 , and D_3 , respectively, lead to sixteen different conformers given in Figure 1.

The Cartesian coordinates of all optimized conformers are given in Table S1 of the Supporting Information. For notation

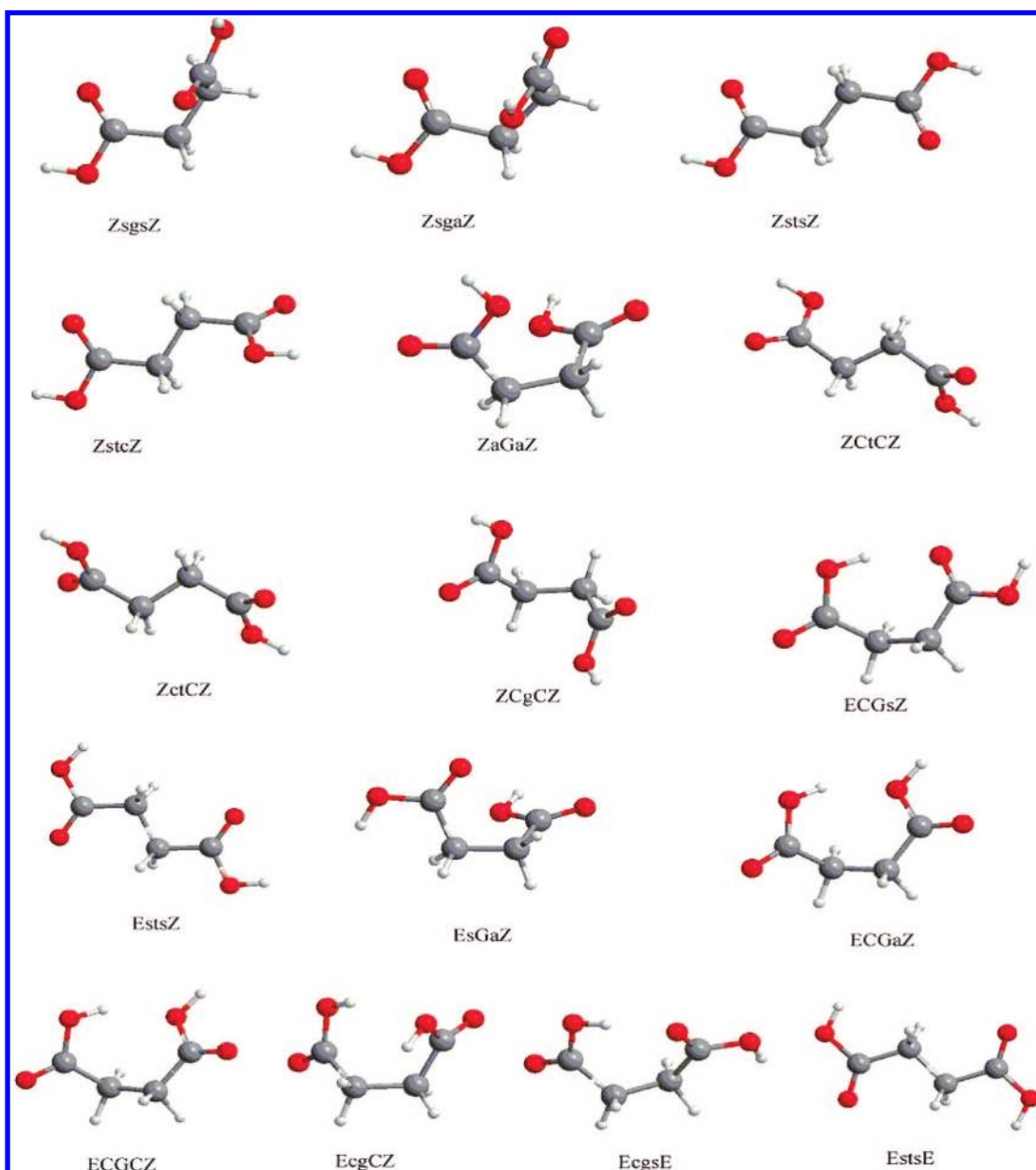


Figure 1. Located isomers of succinic acid calculated at the B3LYP/6-311+G(d,p) level. The ZPE and total energies of predicted conformers calculated at B3LYP/6-311+G(d,p) and G2M(CC2) are given in Table S3.

TABLE 1: Relative Energies (kcal/mol) and Dihedral Angles (deg) D1, D2 and D3 of Predicted Conformers of Succinic Acid, Calculated at the Different Levels of Theory

conformer	B3LYP/6-311+G(d,p)				ΔE		
	ΔE	D1	D2	D3	G2M(CC2)	MP2 ^a	OPLS-AA ^a
ZsgsZ	0.00	11.5	71.9	11.5	0.00	0.00	0.00
ZstsZ	0.02	-3.8	176.3	-3.8	0.75	1.34	1.34
ZsgaZ	1.45	6.6	66.1	-161.5	1.48	1.25	1.29
ZstcZ	1.38	-9.3	175.4	127.5	2.07	2.06	2.12
ZaGaZ	2.69	162.8	-63.0	162.8	2.77	2.50	
ZCtCZ	2.61	-132.5	-179.0	-132.5	3.30	2.93	2.93
ZctCZ	2.88	121.4	180.0	-126.0	3.46	3.15	2.92
ZCgCZ	3.28	-128.9	66.7	-129.1	3.51	2.82	0.99
ECGsZ	3.23	-112.9	-77.5	13.5	3.09	3.76	3.45
EstsZ	5.16	0.0	180.0	0.0	5.10	6.73	8.10
EsGaZ	6.95	-9.0	-66.5	161.2	6.25	8.93	8.52
ECGaZ	6.90	-106.6	-77.9	179.6	7.04	7.04	6.52
ECGCZ	6.89	-118.9	-92.4.0	-144.0	7.31	7.41	6.61
EcgsE	8.67	111.5	77.4	-11.3	7.65	9.41	9.96
EcgCE	16.09	107.8	63.2	-130.6	14.50		
EstsE	10.22	0.0	-180.0	0.0	9.37		

^a MP2 and OPLS-AA data are taken from ref 7.

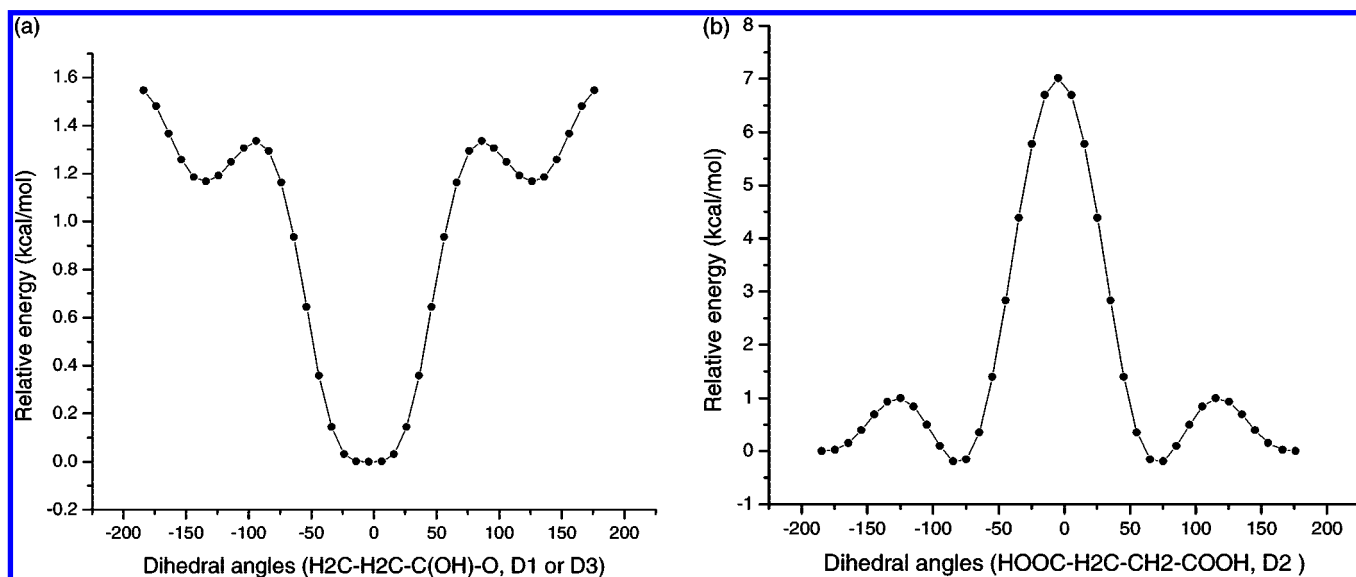
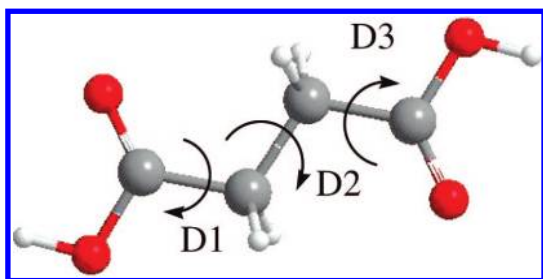


Figure 2. Energy diagram of the reported conformers as a function of dihedral angles (a) D1 or D3, and (b) D2.

SCHEME 1



of these conformers were have adopted the scheme proposed by Price et al.,⁷ which includes five letters as UVWXY. Here, U and Y stand for acid forms of SA and can be *E* or/and *Z* with near 180° and 0° rotational angles (O–C–O–H). V and X stand for angles D1 and D3, respectively, and can be a (anti) and/or s (syn), which stand for structures with near 180° and 0° rotational, D1 and D3, angles or can be c and C that stand for dihedral, D1 and D3, angles near +120° and -120°. W stands for rotational angle D2 and can be g and G indicating structures with near +60° and -60° rotational angles. We also will use (see below) notation t, which stands for trans for the

central dihedral (D2) angle. For example, EsGaZ refers to the diacid conformer (*E* and *Z*) with the O–C–O–H dihedral angle as 180° (*E*) and 0° (*Z*), the D1 and D3 angles as 0° (s, syn) and 180° (a, anti), and the central dihedral (D2) as -60° (G). As seen in Table 1, the ZsgsZ conformer with the two *Z*-acid forms of SA is the most stable structure among the all calculated conformers.

Its ZstsZ and ZsgaZ conformers are calculated to be only 0.75 and 1.48 kcal/mol higher in energy than the most stable ZsgsZ conformer. Additional stabilization of these two *Z*-acid forms of SA dictated by the additional interaction of the lone-pair of oxygen of the COOH group with the σ^* orbital of the central C–C bond. This bonding scheme is supported by comparison of NBO (natural bond orbital) results for ZsgsZ, ZsgaZ, and ZstcZ conformers. As seen in Table 1, the relative energies of all isolated *Z*-acid conformers are within 3.5 kcal/mol. Conformers with mixed (*E* and *Z*) acid forms are grouped within 3.09–7.31 kcal/mol, ECGsZ and ECGCZ being lowest and highest in energy among them, respectively. The located structures, EcgsE, EcgCE and EstsE, with the two *E*-acid forms, are found to be 7.65, 14.50, and 9.37 kcal/mol higher in energy

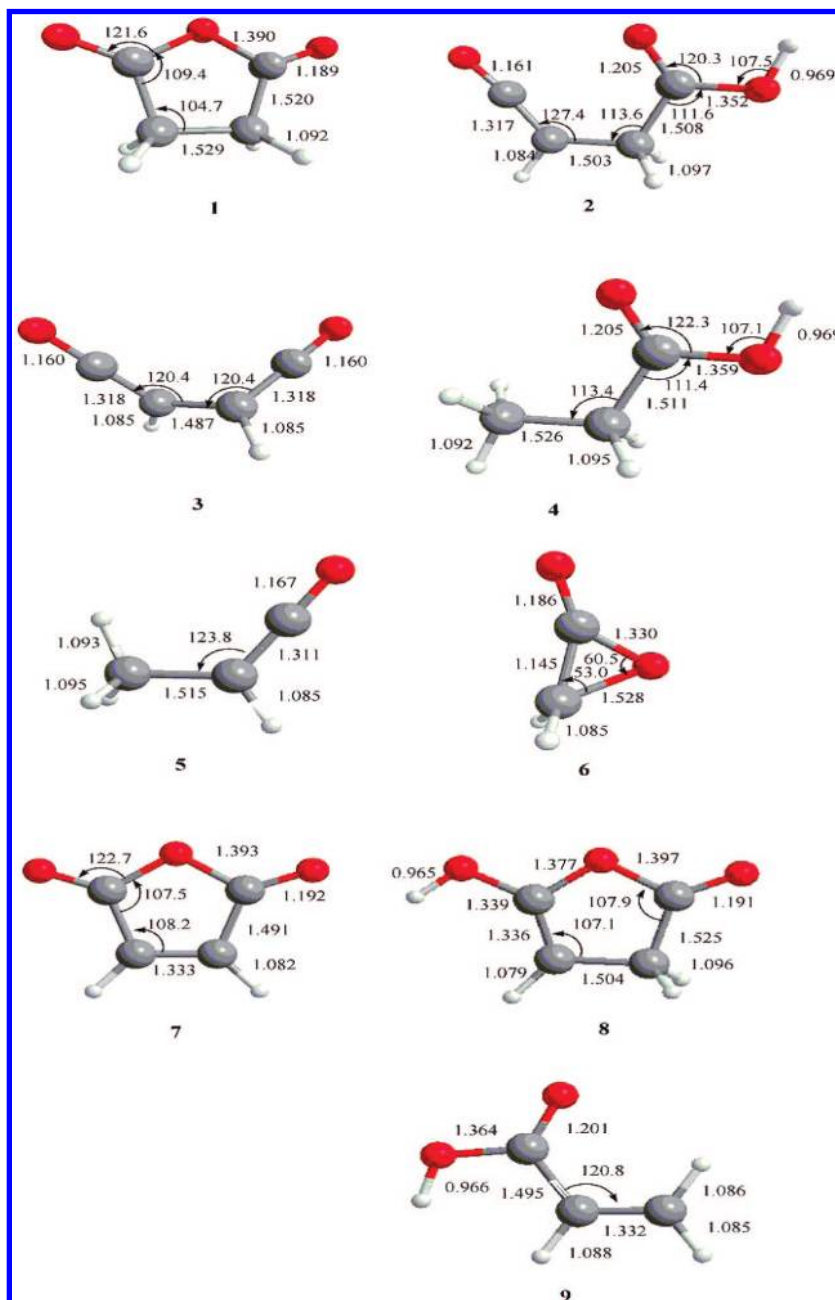


Figure 3. Located intermediates of unimolecular decomposition of succinic acid and its anhydride and their important geometry parameters calculated at the B3LYP/6-311+G(d,p) level of theory.

than ZsgsZ, respectively. Structurally, ECGsZ, ECGaZ, ECGCZ, EcgCZ, and EcgSE (see Figure 1) have an internal hydrogen bond; the H-bonding lengths are 1.847, 1.944, 1.868, 2.333, and 1.845 Å, respectively. Earlier theoretical studies⁷ based on the Hartree–Fock (HF), MP2, and OPLS-AA levels of theory gave consistent results. HF/6-31G(d) calculations predicted ZsgsZ to be 0.59 and 4.86 kcal/mol more stable than ZstsZ and ECGsZ, whereas MP2/6-31G(d)//HF/6-31G(d) and OPLS-AA calculations predicted ZsgsZ to be 1.3 and 3.8, and 1.3 and 3.5 kcal/mol more stable than ZstsZ and ECGsZ, respectively. Our G2M (CC2) results are in good agreement with the high level MP2/6-31G(d)//HF/6-31G(d) and OPLS-AA calculations.

Thus, the Z-acid form of SA is more stable than mixed (*E/Z*)- and *E*-acid forms, which is also observed in acetic acid.¹⁹ The Z-acid form of acetic acid is 4.95 kcal/mol lower than *E*-acid form at the MP2/6-311+G(d,p)//HF/6-31G(d) level of theory.

So, it can be concluded that the *E*-acid conformers of SA will not be significantly populated near room temperature in the gas phase.

To elucidate the conformation mechanisms of SA, we have scanned potential energy surfaces (PES) of the specific processes by changing the corresponding dihedral angles *D*1 (or *D*3), and *D*2 from -180° to $+180^\circ$ by 10° increments. At the each fixed value of the given angle all other geometry parameters were fully optimized. The calculated PES's at the B3LYP/6-311+G(d,p) level are depicted in Figure 2.

As seen from these figures, global minimum on these PESs correspond to 0° and 75° of *D*1 (or *D*3) and *D*2, respectively. These data, once again, show that the ZsgsZ conformer is the most stable one, which is also consistent with the gauche effect.^{20–22} The calculated barriers are 1.33 and 1.54 kcal/mol at 86.1° (or -93.9°) and 176.1° (or -183.9°) for the *D*1 (or

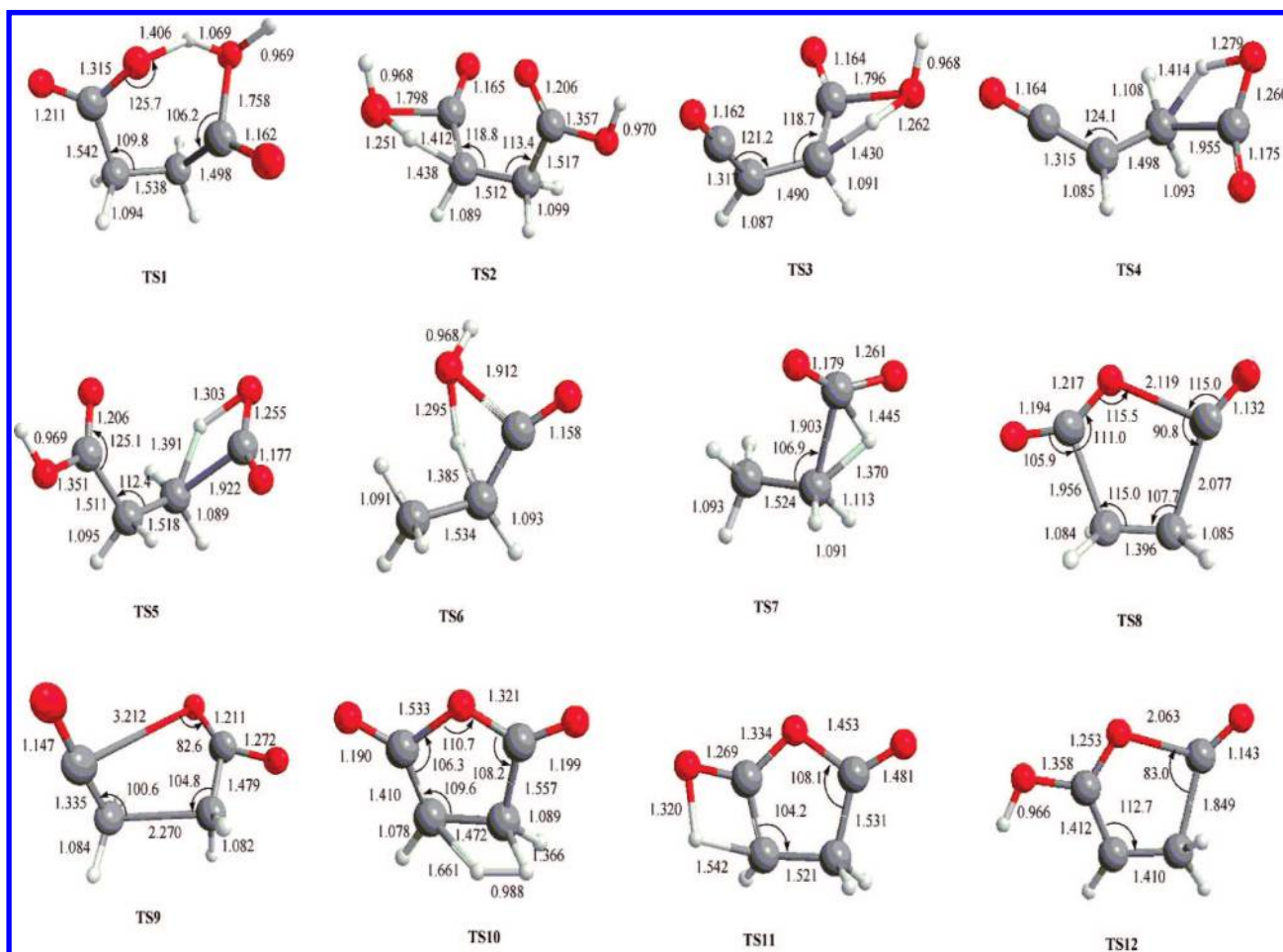


Figure 4. Located transition states of unimolecular decomposition of succinic acid and its anhydride and their important geometry parameters calculated at the B3LYP/6-311+G(d,p) level of theory.

$D3$) rotation; and 0.99 and 7.01 kcal/mol at 115.3° (or -124.7°) and -4.7° for the $D2$ rotation. Thus, the internal rotations around the C–C bond of SA ($D1$, $D2$ and $D3$ rotations) occur easily.

2. Mechanisms for Decomposition of Succinic Acid (SA).

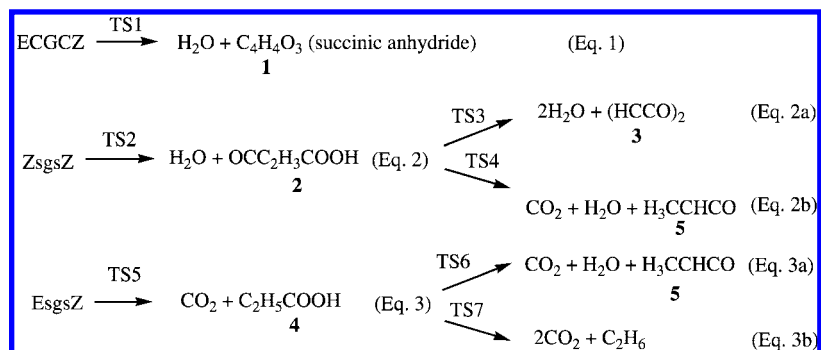
In Figures 3 and 4 we present all intermediates, transition states, and products of the unimolecular succinic acid decomposition. Their calculated geometrical parameters are given in Table S2, and relative energies are schematically presented in Figure 5.

As seen from Scheme 2, the first proposed reaction (eq 1) is a dehydration of SA leading to water molecule and succinic anhydride, which could decompose further (see Scheme 3). The proposed second reaction associates with a subsequent dehydration (eq 2a) and dehydration-then-decarbonylation (eq 2b) mechanisms. The last proposed reaction of unimolecular succinic

acid decomposition is a decarbonylation-then-dehydration (eq 3a) and subsequent decarbonylation (eq 3b) processes. In addition, we compared the available experimental data for the heats of the reactions succinic acid \rightarrow succinic anhydride + H_2O (eq 1) and succinic acid \rightarrow CH_3CH_2COOH + CO_2 (eq 3). The calculated values of +11.3 and -9.7 kcal/mol at 298 K are both in good agreement with the experimental values of $+11.2 \pm 0.02$ and -8.8 ± 0.48 kcal/mol reported by Kistiakowsky et al.^{23a} and NIST thermochemical tables.^{23b}

First, we discuss the dehydration of SA. As seen in Scheme 2, dehydration of SA may start from two different conformers, ECGCZ and Zsgsz, energy difference between which is only 7.0 kcal/mol. Dehydration from the conformer ECGCZ (eq 1) occurs via H-migration from one of the COOH groups to another

SCHEME 2



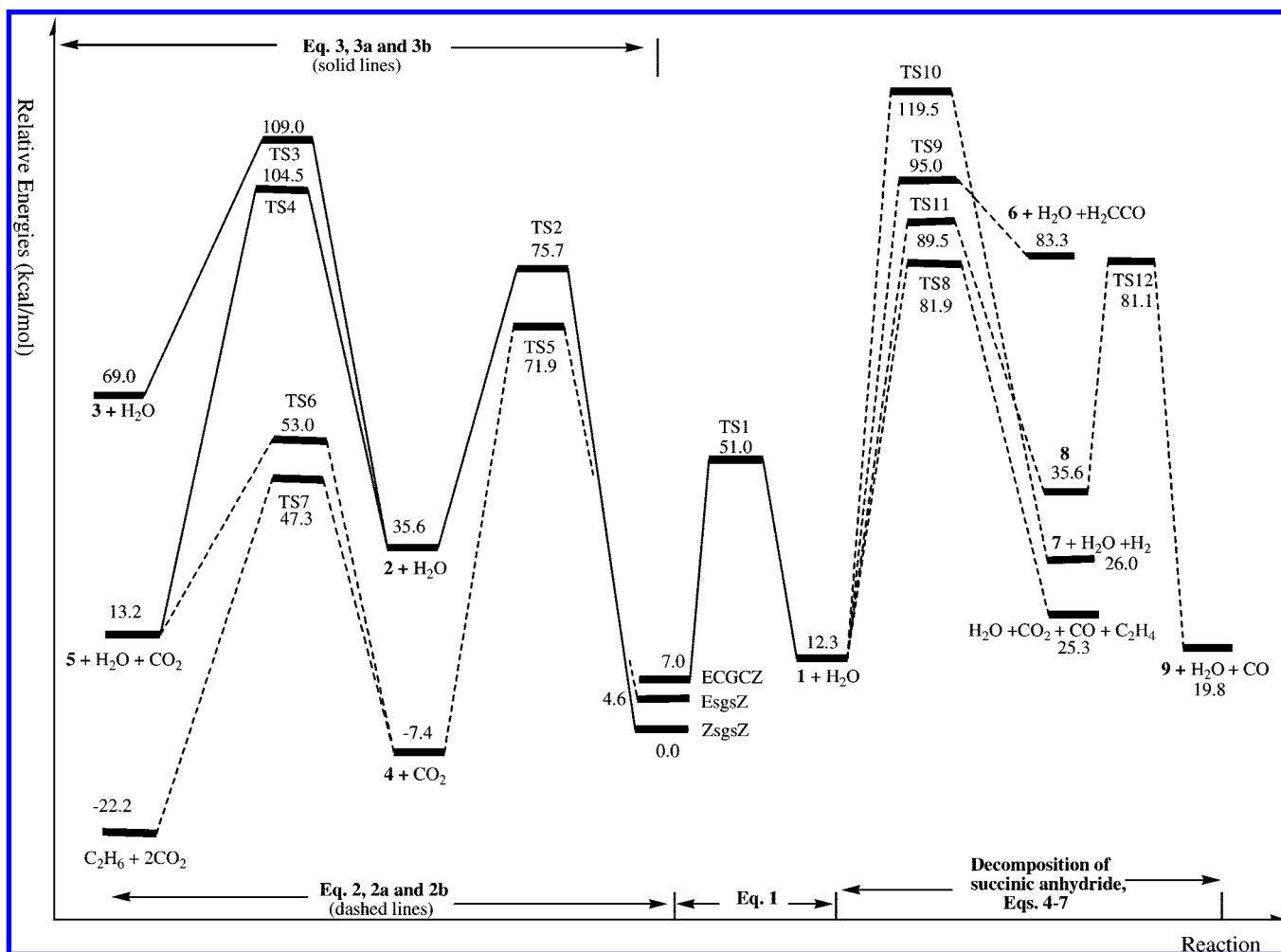


Figure 5. Schematic presentation of energetics of unimolecular decomposition reactions of succinic acid and its anhydride calculated at the G2M(CC2)//B3LYP/6-311+G(d,p) level of theory.

COOH group and leads to formation of cyclic $C_4H_4O_3$ product and water molecule, i.e., intermediate **1** (succinic anhydrite) + H_2O . This process is calculated to be 5.3 kcal/mol endothermic and proceeds with a 44.0 kcal/mol barrier at the concerted transition state TS1 (see Figures 4 and 5). In TS1, the forming C–O bond and the breaking O–H bond are calculated to be 2.181 and 1.406 Å, respectively (Figure 4). The product of this reaction is a cyclic compound $C_4H_4O_3$ (Figure 3).

Energetically, the most stable isomer of SA, ZsgsZ, can also decompose via dehydration pathway (eq 2). As seen in Figures 3–5, dehydration of ZsgsZ leads to formation of OCC_2H_3COOH (intermediate **2**) + H_2O , which occurs via a concerted (simultaneous C–OH bond cleavage and H-migration from CH_2 to OH) transition state TS2. This process is calculated to be endothermic by 35.6 kcal/mol and proceeds with a 75.7 kcal/mol energy barrier. The geometry of the located TS2 is consistent with the nature of the proposed process: In TS2, the bond distances of the breaking HC–H, C–OH bonds and forming HO–H bond are 1.438, 1.798, and 1.251 Å, respectively. Because in the formed intermediate **2** the second CH_2 and COOH fragments are still intact, reaction may follow via a formation of the second water molecule (eq 2a). Calculations show that reaction $2 \rightarrow H_2O + 3$ is also endothermic, by almost the same value as the first dehydration process (from the ZsgsZ), 33.4 kcal/mol, and occurs with a 78.4 kcal/mol barrier. Thus, the subsequent dehydration of SA is an additive process. Overall double dehydration of SA, $ZsgsZ \rightarrow 2H_2O + 3$, requires 109.0 kcal/mol barrier and is endothermic by 69 kcal/mol.

The intermediate **2**, product of the first dehydration of ZsgsZ, may also undergo decarboxylation to form CO_2 and intermediate **5** (eq 2b). As seen in Figure 5, in fact, decarboxylation of **2** is slightly more favorable than its dehydration. Indeed, decarboxylation of **2** is found to proceed with a 68.9 kcal/mol barrier at transition state TS4, and is 22.4 kcal/mol exothermic to give $CO_2 + H_3CCHCO$ (**5**) products. Overall dehydration followed by decarboxylation (i.e., dehydration-then-decarboxylation, eq 2b) of SA, $ZsgsZ \rightarrow H_2O + CO_2 + H_3CCHCO$ (**5**), is found to be endothermic by 13.2 kcal/mol, and proceeds with 104.5 kcal/mol barrier at TS4.

Now, we discuss the mechanism of SA decomposition via the decarboxylation pathway (eq 3). This process involves migration of H from COOH-fragment to CH_2 . It starts from EsgsZ conformer of SA (which is a 4.6 kcal/mol higher in energy than the most stable conformer ZsgsZ) and leads to C_2H_5COOH (**4**) and CO_2 . It occurs via a TS5, where simultaneously HOOC– CH_2 bond cleaves and H migrates from the COOH fragment to CH_2 . As seen in Figure 4, in TS5, the forming C–H bond and the breaking O–H and C–C bonds are 1.391, 1.303, and 1.922 Å, respectively. The barrier associated with this transition state is 71.9 kcal/mol. Reaction $EsgsZ \rightarrow CO_2 + C_2H_5COOH$ (**4**) is found to be exothermic by 7.4 kcal/mol. From the formed intermediate **4** reaction may proceed via two different pathways: dehydration (called as decarboxylation-then-dehydration, eq 3a) and decarboxylation (the formation of the second carbonyl dioxide, eq 3b). The first pathway occurs via transition state TS6 and associated 60.4 kcal/

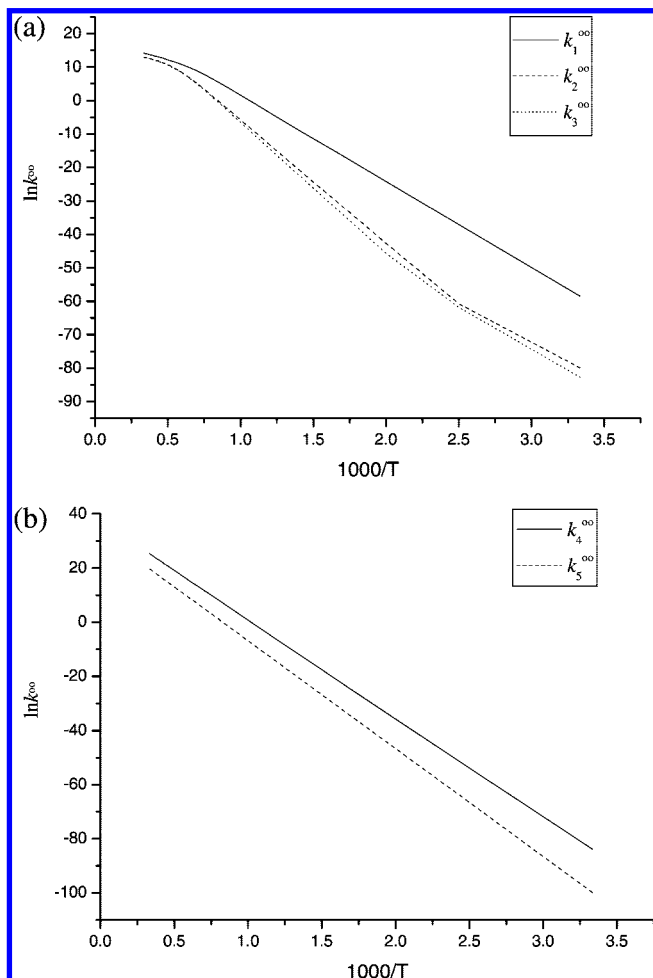


Figure 6. Predicted first-order rate constants (in unit of s^{-1}) in the temperature range 300–3000 K for decomposition of (a) succinic acid (k_1^∞ , k_2^∞ , and k_3^∞) and (b) succinic anhydride (k_4^∞ , and k_5^∞).

mol barrier and leads to $H_2O + H_3CCHCO$ (**5**) products. This process is found to be a 20.6 kcal/mol endothermic. However, decarbonylation of C_2H_5COOH (**4**) occurs with a slightly less barrier, 54.7 kcal/mol, at transition state TS7, and is exothermic by 14.8 kcal/mol.

Thus, the above-presented results clearly show that direct dehydration and decarbonylation of the energetically lowest conformer of SA, ZsgsZ, is kinetically and thermodynamically less favorable. However, it can easily rearrange to excited conformers, such as ECGCZ and EsgsZ, which decompose relatively easier via the dehydration (to lead succinic anhydride) and decarbonylation (to lead $2CO_2 + C_2H_6$ products) pathways. The first channel (eq 1), dehydration of SA with formation of **1** (succinic anhydride) and H_2O molecule looks kinetically and thermodynamically more favorable. Therefore, below, we study the processes starting from the intermediate **1** (succinic anhydride) in more details.

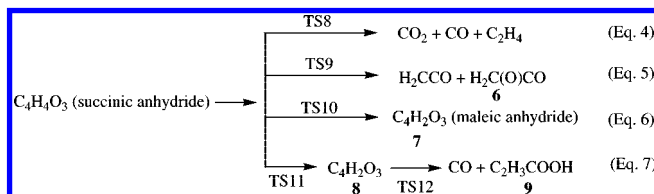
As mentioned above, the decomposition mechanism of C_2H_5COOH involves two channels: (1) dehydration (giving $H_3CCHCO + H_2O$; eq 3a) and (2) dehydrogenation (giving $C_2H_6 + CO_2$; eq 3b). The effect of quantum-mechanical tunneling on the decomposition reactions has been considered. The predicted rate constants for the unimolecular dehydration and decarboxylation processes in the temperature range 700–1000 K at 100 Torr average experimental pressure are given by $k_{3a} = 1.52 \times 10^9 \exp(-48.86 \text{ cal mol}^{-1}/RT) s^{-1}$ and $k_{3b} = 5.12 \times 10^9 \exp(-44.17 \text{ cal mol}^{-1}/RT) s^{-1}$. Our results are in good

agreement with the experimental values for both product channels.²⁴ The predicted overall activation energy is 44.2 kcal/mol is in excellent agreement with experimental value of 43.3 kcal/mol.²⁴

3. Mechanisms for Decomposition of Succinic Anhydride,

1. On the basis of our extensive preliminary analysis, we have proposed four decomposition pathways for succinic anhydride (Scheme 3).

SCHEME 3



First of them is the pathway leading to $C_2H_4 + CO_2 + CO$ products. This reaction occurs with a concerted five-membered transition state, TS8, where the breaking C–C and C–O bonds are 1.956, 2.077, and 2.119 Å, respectively. The barrier associated with this transition state is 69.6 kcal/mol. The overall reaction $\mathbf{1} \rightarrow C_2H_4 + CO_2 + CO$ is found to be endothermic by 13.0 kcal/mol. The second proposed decomposition pathway of succinic anhydride leads to the H_2CCO and cyclic $H_2C(O)CO$ intermediate **6**. It proceeds through TS9. Energy barrier associated with this transition state is 82.7 kcal/mol barrier. The entire reaction $\mathbf{1} \rightarrow H_2CCO + H_2C(O)CO$ (**6**) is found to be endothermic by 71.0 kcal/mol. As seen in Figure 4, at transition state TS9, breaking C–C and C–O bonds are elongated to 2.270 and 3.212 Å, respectively. The third proposed pathway is a dehydrogenation reaction leading to formation of the maleic anhydride, intermediate **7** ($C_4H_2O_3$) and dihydrogen molecule. This process occurs with a high-energy barrier (107.2 kcal/mol) at transition state TS10 and is 13.7 kcal/mol endothermic. As seen in Figure 4, the forming H_2 molecule results from the $H_2C=CH_2$ unit: the breaking C–H bonds are 1.661 Å and the forming H–H bond distance is 0.988 Å in transition state TS10.

The first step of the last (fourth) proposed channel for succinic anhydride decomposition is the H-migration from the CH_2 -group to the CO-unit to form intermediate **8**, $C_4H_4O_3$ with a terminal OH-group. The calculated barrier for this H-migration process is found to be a 77.2 kcal/mol at transition state TS11. The resulting reaction $\mathbf{1} \rightarrow \mathbf{8}$ is endothermic by 23.3 kcal/mol. At the next stage, intermediate **8** decomposes to C_2H_3COOH (**9**) + CO via a barrier of 45.5 kcal/mol at transition state TS12. Thus, the overall reaction $\mathbf{1} \rightarrow \mathbf{8} \rightarrow C_2H_3COOH$ (**9**) + CO occurs with a 77.2 kcal/mol barrier at TS11 and is endothermic by 7.5 kcal/mol.

Thus, on the basis of the above-presented discussion (Figure 5), the kinetically and energetically most visible channels of succinic anhydride decomposition are those leading to $CO_2 + CO + C_2H_4$ and C_2H_3COOH (**9**) + CO, which proceed by 69.6 and 77.2 kcal/mol rate-limiting barriers, and are endothermic by 13.0 and 7.5 kcal/mol, respectively.

4. Rate Constant Calculations. The microcanonical Rice–Ramsperger–Kassel–Marcus (RRKM) theory was employed to calculate the rate constants for the unimolecular decomposition of SA and its anhydride. The effect of quantum-mechanical tunneling on the decomposition reactions have been considered (on the basis of the Eckart model implemented in the ChemRate program¹⁸). The moments of inertia and vibrational frequencies of reactants and transition states presented in Table S2 were

used. The Lennard-Jones (L-J) parameters employed for the succinic acid decomposition reaction are as follows: Ar, $\sigma = 4.42 \text{ \AA}$, $\epsilon/k = 164 \text{ K}$ and succinic acid, $\sigma = 5.30 \text{ \AA}$, $\epsilon/k = 676 \text{ K}$. For the succinic anhydride system they are as follows: Ar, $\sigma = 4.33 \text{ \AA}$, $\epsilon/k = 171 \text{ K}$ and succinic anhydride, $\sigma = 5.12 \text{ \AA}$, $\epsilon/k = 735 \text{ K}$ using the formulas ($\epsilon/k = 0.897T_c$, $\sigma = 0.785V_c^{1/3}$).²⁵ The energy-transfer process was computed on the basis of the exponential down model with a $\langle \Delta E \rangle_{\text{down}}$ value (the mean energy transferred per collision) of 400 cm^{-1} for Ar. The multichannel models were used in the rate constant calculations.

As shown in the PES, the decomposition channels of SA takes place by the eqs 1, 2, and 3 shown in Scheme 2, for which the rate constants are controlled by the well-defined TS1, TS2, and TS5, respectively. Figure 6 displays the predicted rate constants of k_1^∞ , k_2^∞ and k_3^∞ in the temperature range 300–3000 K. The results show that the thermal decomposition of SA should be dominated by the dehydration process to produce the succinic anhydride in the whole temperature range. At the high pressure, the thermal decomposition rate constant including the contributions from other conformers of succinic acid defined by

$$d[\text{C}_4\text{H}_4\text{O}_3]/dt = k^\infty[(\text{CH}_2\text{COOH})_2]_0 = \sum k_i^\infty X_i = k_x^\infty [\text{X}] + k_A^\infty [\text{A}] + k_B^\infty [\text{B}] + \dots + k_O^\infty [\text{O}]$$

where $[(\text{CH}_2\text{COOH})_2]_0$, $[\text{X}]$, $[\text{A}]$, $[\text{B}]$, ..., $[\text{O}]$ are the initial concentration of ZsgsZ, ZstsZ, ZsgaZ, ..., EstsE, respectively, under thermal equilibrium, and the k_i^∞ are the first-order rate constant for the decomposition from these conformers. Assuming K_A , K_B , ..., and K_O to be the equilibrium constant for ZsgsZ \rightarrow ZstsZ, ZsgsZ \rightarrow ZsgaZ, ..., ZsgsZ \rightarrow EstsE, respectively, leads to the total rate constant:

$$k^\infty = (k_x + k_A K_A + k_B K_B + \dots + k_O K_O) / (1 + K_A + K_B + \dots + K_O)$$

The rate constants for these key decomposition reactions have been calculated for 1 and 100 atm, and the high-pressure limit in the temperature range 300–3000 K is expressed as the following equations:

$$k_1^{1\text{atm}} = 2.77 \times 10^{14} T^{-0.00371} \exp(-53.88 \text{ kcal mol}^{-1}/RT) \text{ s}^{-1}$$

$$k_1^{100\text{atm}} = 3.28 \times 10^{13} T^{-0.0172} \exp(-52.93 \text{ kcal mol}^{-1}/RT) \text{ s}^{-1}$$

$$k_1^\infty = 3.31 \times 10^{13} T^{-0.00272} \exp(-53.04 \text{ kcal mol}^{-1}/RT) \text{ s}^{-1}$$

$$k_2^{1\text{atm}} = 3.17 \times 10^{14} T^{-0.00453} \exp(-72.75 \text{ kcal mol}^{-1}/RT) \text{ s}^{-1}$$

$$k_2^{100\text{atm}} = 4.01 \times 10^{13} T^{-0.00137} \exp(-69.38 \text{ kcal mol}^{-1}/RT) \text{ s}^{-1}$$

$$k_2^\infty = 1.42 \times 10^{13} T^{-0.00157} \exp(-68.36 \text{ kcal mol}^{-1}/RT) \text{ s}^{-1}$$

$$k_3^{1\text{atm}} = 5.41 \times 10^{14} T^{-0.00452} \exp(-70.32 \text{ kcal mol}^{-1}/RT) \text{ s}^{-1}$$

$$k_3^{100\text{atm}} = 2.60 \times 10^{13} T^{-0.00115} \exp(-71.98 \text{ kcal mol}^{-1}/RT) \text{ s}^{-1}$$

$$k_3^\infty = 1.15 \times 10^{13} T^{-0.00132} \exp(-70.04 \text{ kcal mol}^{-1}/RT) \text{ s}^{-1}$$

The overall rate constants for succinic acid decomposition should be expressed as

$$k_{1+2+3}^{1\text{atm}} = 2.76 \times 10^{14} T^{-0.0037} \exp(-53.88 \text{ kcal mol}^{-1}/RT) \text{ s}^{-1}$$

$$k_{1+2+3}^{100\text{atm}} = 3.89 \times 10^{13} T^{-0.00162} \exp(-52.87 \text{ kcal mol}^{-1}/RT) \text{ s}^{-1}$$

$$k_{1+2+3}^\infty = 2.27 \times 10^{13} T^{-0.00241} \exp(-52.85 \text{ kcal mol}^{-1}/RT) \text{ s}^{-1}$$

In addition, the following decomposition channels of the succinic anhydride produce $\text{CO} + \text{CO}_2 + \text{C}_2\text{H}_4$ (eq 4) and $\text{CO} + \text{C}_2\text{H}_3\text{COOH}$ (eq 7) as also shown in Figure 4 and Scheme 3. The decomposition rate constant of succinic anhydride in the temperature range 300–3000 K can be given as follows:

$$k_4^{1\text{atm}} = 1.35 \times 10^{17} T^{-0.00527} \exp(-68.42 \text{ kcal mol}^{-1}/RT) \text{ s}^{-1}$$

$$k_4^{100\text{atm}} = 1.62 \times 10^{17} T^{-0.00364} \exp(-691 \text{ kcal mol}^{-1}/RT) \text{ s}^{-1}$$

$$k_4^\infty = 1.68 \times 10^{16} \exp(-72.23 \text{ kcal mol}^{-1}/RT) \text{ s}^{-1}$$

$$k_5^{1\text{atm}} = 6.36 \times 10^{13} T^{-0.00225} \exp(-72.93 \text{ kcal mol}^{-1}/RT) \text{ s}^{-1}$$

$$k_5^{100\text{atm}} = 3.62 \times 10^{12} T^{-0.00006} \exp(-71.39 \text{ kcal mol}^{-1}/RT) \text{ s}^{-1}$$

$$k_5^\infty = 2.14 \times 10^{14} \exp(-78.90 \text{ kcal mol}^{-1}/RT) \text{ s}^{-1}$$

The overall rate constants for succinic anhydride decomposition should be expressed as

$$k_{4+5}^{1\text{atm}} = 1.30 \times 10^{17} T^{-0.0009} \exp(-68.09 \text{ kcal mol}^{-1}/RT) \text{ s}^{-1}$$

$$k_{4+5}^{100\text{atm}} = 1.58 \times 10^{17} T^{-0.00016} \exp(-68.98 \text{ kcal mol}^{-1}/RT) \text{ s}^{-1}$$

$$k_{4+5}^\infty = 1.68 \times 10^{16} \exp(-72.23 \text{ kcal mol}^{-1}/RT) \text{ s}^{-1}$$

Conclusions

The conformational analysis and unimolecular decomposition mechanisms of succinic acid (SA) as well as its anhydride have been studied at the G2M (CC2) level of theory. The microcanonical RRKM method was applied to calculate the kinetics of the studied unimolecular decomposition processes. The relative energies of all isolated Z-acid conformers are within 3.5 kcal/mol, the ZsgsZ conformer with the gauche conformation around the central C–C bond is its most stable conformer. Conformers with mixed (*E* and *Z*) acid forms are grouped within 3.09–7.31 kcal/mol, with ECGsZ and ECGCZ being the lowest and highest in energy among them, respectively. The located three *E*-acid form structures, EcgsE, EcgCE, and EstsE, are found to be 7.65, 14.50, and 9.37 kcal/mol higher in energy than ZsgsZ, respectively. For the succinic acid decomposition, the dehydration process ($\text{H}_2\text{O} + \text{succinic anhydride}$) starting from the ECGCZ-conformer is found to be dominant, whereas the decarboxylation reaction ($\text{CO}_2 + \text{C}_2\text{H}_5\text{COOH}$) starting from the ZsgsZ-conformer is only slightly less favorable. In addition, the decomposition of its anhydride takes place via a concerted fragmentation mechanism (with a 69.6 kcal/mol barrier) leading to formation of $\text{CO} + \text{CO}_2 + \text{C}_2\text{H}_4$ products. The rate constants for unimolecular decomposition of succinic acid and its anhydride have been computed in the temperature range 300–3000 K. The predicted rate constants may be employed for practical applications.

Acknowledgment. We gratefully acknowledge: (1) financial support from the Office of Naval Research under a MURI grant

(Prime Award # N00014-04-1-0683 and Subaward # 2794-EU-ONR-0683), (2) the Emerson Center for the use of its resources, and (3) the use of CPU's from National Center for High-performance Computing, Taiwan. M.C.L. acknowledges the support from National Science Council of Taiwan for this distinguished visiting professorship. J.-G.C. acknowledges the financial support from the Emerson Center Visiting Fellowship of Emory University.

Supporting Information Available: Complete ref 13. **Table S1**, Cartesian coordinates of all optimized isomers of succinic acid; **Table S2**, calculated Cartesian coordinates of intermediates, transition states and products of the unimolecular succinic acid and its anhydride decomposition; **Table S3**, ZPE and total energies of all conformers calculated at B3LYP/6-311+G(d,p) and G2M(CC2); **Table S4**, frequencies and moments of inertia I_i of the decomposition reaction of succinic acid and succinic anhydride calculated at the B3LYP/6-311+G(d,p) level. This material is available free of charge via the Internet at <http://pubs.acs.org>.

References and Notes

- (1) Zeikus, J. G.; Jain, M. K.; Elankovan, P. *Appl. Microbiol. Biotechnol.* **1999**, *51*, 545.
- (2) Grosjean, D.; van Cauwenberghe, K.; Schmid, J. P.; Kelley, P. E.; Pitts, J. *Environ. Sci. Technol.* **1978**, *12*, 313.
- (3) Dockery, D. W.; Pope, C. A. *Annu. Rev. Public Health* **1994**, *15*, 107.
- (4) Stott, P. A.; Tett, S. F. B.; Jones, G. S.; Allen, M. R.; Mitchell, J. F. B.; Jenkins, G. J. *Science* **2000**, *290*, 2133.
- (5) Song, H.; Lee, S. Y. *Enzyme Microbiol. Technol.* **2006**, *39*, 352.
- (6) Kuo, K. K.; Acharya, R.; Boyd, E.; Thynell, S. T. Pyrolysis Study of SA/PVA as Ablative Material for Boundary Layer Control System in High-pressure Graphite Rocket Nozzle; AIAA/ASME/SAE/ASEE Joint Propulsion Conference, 2007.
- (7) Price, D. J.; Roberts, J. D.; Jorgensen, W. L. *J. Am. Chem. Soc.* **1998**, *120*, 9672.
- (8) Becke, A. D. *J. Chem. Phys.* **1992**, *96*, 2155.
- (9) Becke, A. D. *J. Chem. Phys.* **1992**, *97*, 9173.
- (10) Becke, A. D. *J. Chem. Phys.* **1993**, *98*, 564.
- (11) Gonzalez C. Schlegel H. B. *J. Chem. Phys.* **1989**, *90*, 2154; *J. Phys. Chem.* **1990**, *94*, 5523.
- (12) Mebel, A. M.; Morokuma, K.; Lin, M. C. *J. Chem. Phys.* **1995**, *103*, 7414.
- (13) Frisch, M. J.; et al. *Gaussian 03*, revision C.02; Gaussian, Inc., Wallingford, CT, 2004.
- (14) Klippenstein, S. J. *J. Chem. Phys.* **1992**, *96*, 367.
- (15) Klippenstein, S. J.; Marcus, R. A. *J. Chem. Phys.* **1987**, *87*, 3410.
- (16) Wardlaw, D. M.; Marcus, R. A. *Chem. Phys. Lett.* **1984**, *110*, 230.
- (17) Wardlaw, D. M.; Marcus, R. A. *J. Chem. Phys.* **1985**, *83*, 3462.
- (18) Mokrushin, W. B., V.; Tsang, W.; Zachariah, M.; Knyazev, V. *ChemRate*, version 1.5.2 ed.; National Institute of Standards and Technology: Gaithersburg, MD, 2006.
- (19) Rablen, P. R. Personal communication.
- (20) Alemán, C.; Puiggali, J. *J. Org. Chem.* **1997**, *62*, 3076.
- (21) Wiberg, K. B. *Acc. Chem. Res.* **1996**, *29*, 229.
- (22) Wolfe, S. *Acc. Chem. Res.* **1972**, *5*, 102.
- (23) (a) Conn, J. B.; Kistiakowsky, G. B.; Roberts, R. M.; Smith, E. A. Heats of organic reactions. XIII. Heats of hydrolysis of some acid anhydrides. *J. Am. Chem. Soc.* **1942**, *64*, 1747. (b) The heats of formation at 298 K for succinic anhydride and $\text{CH}_3\text{CH}_2\text{COOH}$, -126.2 ± 0.41 and -108.9 ± 0.48 kcal/mol, are taken from the NIST website: <http://www.nist.gov/>.
- (24) Blake, P. G.; Hole, K. J. *J. Chem. Soc. B* **1966**, 577.
- (25) Mourits, F. M.; Rummens, F. H. A. *Can. J. Chem.* **1977**, *55*, 3007.

JP8019733